THE JOURNAL OF BIOLOGICAL CHEMISTRY VOL. 292, NO. 9, pp. 3789–3799, March 3, 2017

Janus Kinase 2 (JAK2) Dissociates Hepatosteatosis from Hepatocellular Carcinoma in Mice*[S]

Received for publication, August 7, 2016, and in revised form, December 29, 2016 Published, JBC Papers in Press, January 18, 2017, DOI 10.1074/jbc.M116.752519

Sally Yu Shi[‡§1], Cynthia T. Luk[‡§2,3], Stephanie A. Schroer[‡2], Min Jeong Kim[‡¶2], David W. Dodington[‡], Tharini Sivasubramaniyam[‡§1], Lauren Lin[‖], Erica P. Cai[‡§], Shun-Yan Lu[‡], Kay-Uwe Wagner[**], Richard P. Bazinet[‖], and Minna Woo[‡§‡‡4]

From the [‡]Toronto General Hospital Research Institute, Toronto, Ontario M5G 2C4, Canada, the [§]Institute of Medical Science, University of Toronto, Toronto, Ontario M5S 1A8, Canada, the [¶]Institute of Medical Research, Kangbuk Samsung Hospital, Sungkyunkwan University School of Medicine, Seoul 03181, Korea, the [‖]Department of Nutritional Sciences, University of Toronto, Toronto, Ontario M5S 3E2, Canada, the [**]Eppley Institute for Research in Cancer and Allied Diseases and the Department of Pathology and Microbiology, University of Nebraska Medical Center, Omaha, Nebraska 68198-6805, and the [‡‡]Division of Endocrinology, Department of Medicine, Toronto General Hospital, University Health Network, University of Toronto, Toronto, Ontario M5G 1L7, Canada

Edited by Eric R. Fearon

Hepatocellular carcinoma is an end-stage complication of non-alcoholic fatty liver disease (NAFLD). Inflammation plays a critical role in the progression of non-alcoholic fatty liver disease and the development of hepatocellular carcinoma. However, whether steatosis *per se* promotes liver cancer, and the molecular mechanisms that control the progression in this disease spectrum remain largely elusive. The Janus kinase signal transducers and activators of transcription (JAK-STAT) pathway mediates signal transduction by numerous cytokines that regulate inflammation and may contribute to hepatocarcinogenesis. Mice with hepatocyte-specific deletion of JAK2 (L-JAK2 KO) develop extensive fatty liver spontaneously. We show here that this simple steatosis was insufficient to drive carcinogenesis. In fact, L-JAK2 KO mice were markedly protected from chemically induced tumor formation. Using the methionine choline-deficient dietary model to induce steatohepatitis, we found that steatohepatitis development was completely arrested in L-JAK2 KO mice despite the presence of steatosis, suggesting that JAK2 is the critical factor required for inflammatory progression in the liver. In line with this, L-JAK2 KO mice exhibited attenuated inflammation after chemical carcinogen challenge. This was associated with increased hepatocyte apoptosis without elevated compensatory proliferation, thus thwarting expansion of transformed hepatocytes. Taken together, our findings identify an indispensable role of JAK2 in hepatocarcinogenesis through regulating critical inflammatory pathways. Targeting the JAK-STAT pathway may provide a novel therapeutic option for the treatment of hepatocellular carcinoma.

Primary liver cancer, consisting predominantly of hepatocellular carcinoma, currently represents the fifth most common cancer in the world and the third leading cause of cancer-related deaths (1). Over the last two decades, the incidence of liver cancer in developed countries has increased dramatically due to the growing prevalence of its risk factors, including chronic infections with hepatitis B or C virus and, more recently, obesity and non-alcoholic fatty liver disease (NAFLD) (1).

Fatty liver disease often occurs on a background of obesity and insulin resistance and has become the most common form of chronic liver disease in developed countries. Non-alcoholic fatty liver disease encompasses a spectrum of disorders ranging from simple steatosis with a non-progressive clinical course to non-alcoholic steatohepatitis, characterized by chronic inflammation, hepatocyte damage, and varying degrees of fibrosis (2, 3). Non-alcoholic steatohepatitis significantly increases the risk of cirrhosis and hepatocellular carcinoma (4, 5). To date, the exact mechanisms underlying non-alcoholic steatohepatitis progression and hepatocellular carcinoma development remain elusive.

In the setting of hepatic steatosis, the progressive intracellular deposition of lipids is thought to sensitize the liver to a secondary insult, resulting in inflammatory activation (6). In particular, lipid accumulation induces oxidative damage, promoting DNA damage and genomic instability (7). Activation of the inflammatory response leads to hepatocellular injury, inducing cell death and promoting compensatory proliferation of damaged hepatocytes. This chronic cycle of cell injury, inflammation, and regeneration contributes to the development of hepatocellular carcinoma (8–10). Therefore, chronic inflammation plays a critical role in the initiation and promotion of liver tumorigenesis. Indeed, in animal models,

* This work was supported by Canadian Institute of Health Research (CIHR) Operating Grant MOP-142193, a Canadian Cancer Society Innovation Grant, and by a Canadian Diabetes Association (CDA) grant-in-aid (to M. W.), The authors declare that they have no conflicts of interest with the contents of this article.
[S] This article contains supplemental Figs. S1–S7.
[1] Supported by a CIHR Doctoral Research Award, a CDA Doctoral Student Research Award, and a Canadian Liver Foundation Graduate Studentship.
[2] These authors contributed equally to this work.
[3] Supported by the Eliot Phillipson Clinician Scientist Training Program, a CDA Postdoctoral Fellowship, and a Banting and Best Diabetes Centre Postdoctoral Fellowship.
[4] Supported by the Canada Research Chair in Signal Transduction in Diabetes Pathogenesis. To whom correspondence should be addressed: Toronto General Hospital Research Institute, 101 College St., MaRS Centre/TMDT, Rm. 10-363, Toronto, Ontario, Canada M5G 1L7. Tel.: 416-581-7531; Fax: 416-581-7880; E-mail: mwoo@uhnresearch.ca.

genetically or chemically induced hepatocellular carcinoma has been shown to depend on inflammatory signaling (11–14). Nevertheless, whether lipid accumulation *per se* promotes neoplasia remains largely elusive. The relative contribution of individual molecular players in the inflammatory response to disease progression is also not fully understood.

The Janus kinase-signal transducers and activators of transcription (JAK-STAT) pathway is one of the major signaling cascades that mediates cytokine-induced inflammatory response. JAK2, a ubiquitously expressed member in the JAK family, is activated by several cytokines and growth factors in the liver, most notably growth hormone, prolactin, IFN-γ, leptin, and the IL-6 family of cytokines (15). Consistent with its role in mediating inflammatory cytokine signaling, chemical inhibition of JAK2 protected mouse liver from inflammation and apoptosis induced by ischemia and reperfusion (16). Signals through JAK2 are transduced by STAT proteins, which have well known effects on inflammation and tumor development. STAT1 increases anti-tumor immunity, whereas STAT3, and to a lesser extent STAT5, enhances tumor-promoting inflammation, increases cellular proliferation, and suppresses apoptosis, thus promoting cellular transformation (17). However, the exact contribution of JAK2 to development of non-alcoholic steatohepatitis and progression to hepatocellular carcinoma has not been fully elucidated. We and others have recently shown that mice with hepatocyte-specific deletion of JAK2 (L-JAK2 KO) develop fatty liver spontaneously on a regular chow diet (18, 19). Interestingly, despite the profound steatosis, JAK2 disruption did not predispose to steatohepatitis development even on a high fat diet (18), implicating a critical role of JAK2 in the inflammatory progression of non-alcoholic fatty liver disease.

In this study, to investigate the role of JAK2 in hepatocarcinogenesis, we employed a chemically induced hepatocellular carcinoma model using the carcinogen diethylnitrosamine (DEN).[5] Surprisingly, L-JAK2 KO mice were protected from DEN-induced liver tumor development despite extensive lipid accumulation. This was associated with increased hepatocyte apoptosis but not cellular proliferation. To assess whether JAK2 is involved in the inflammatory progression of fatty liver disease, we employed the methionine-choline deficient (MCD) diet, a well established murine dietary model for the study of non-alcoholic steatohepatitis (20, 21). Using this model, we found that despite significant hepatic steatosis on chow diet, L-JAK2 KO mice were protected from further lipid accumulation induced by an MCD diet. Accordingly, whereas the MCD diet provoked hepatic inflammatory activation and progression to fibrosis in control mice, steatohepatitis development was completely arrested in L-JAK2 KO mice.

Results

Hepatic JAK2 Deficiency Protects from Chemical Carcinogenesis—We used the chemical procarcinogen DEN, which induces hepatocellular carcinoma formation after administration to juvenile mice due to the high proliferation rate of hepatocytes at the young age (22). This model of DEN-induced hepatocellular carcinoma is dependent on inflammation and bears genetic and histological similarities with human hepatocellular carcinomas that have a poor prognosis (23). We administered DEN (25 mg/kg) to mice at postnatal day 14, and tumor analysis was conducted at 10 months of age. To investigate if JAK2 is involved in hepatocarcinogenesis, we first evaluated JAK2 activation in liver tumor tissue. Increased JAK2 phosphorylation was observed in tumor compared with non-tumor tissue from wild-type mice injected with DEN, with no change in total JAK2 (Fig. 1*A*, supplemental Fig. S1*A*), suggesting that hepatic JAK2 signaling is activated in the setting of tumorigenesis. Next, to determine the significance of JAK2 in the development of liver cancer, we used mice with hepatocyte-specific JAK2 deficiency (L-JAK2 KO) generated previously (18). Consistent with previous reports, L-JAK2 KO mice had lower body weight than littermate controls throughout the monitoring period (supplemental Figs. S1*B* and S2*A*), with markedly blunted IGF-1 levels in the circulation (supplemental Fig. S1*C*). Serum growth hormone (GH) levels, on the other hand, were not significantly altered (supplemental Fig. S1*C*). When analyzed at 10 months of age, male L-JAK2 KO mice showed reduced liver weight despite extensive intrahepatic lipid accumulation (Fig. 2, *A–C*, and supplemental Fig. S1*D*). Although all mice treated with DEN developed hepatocellular carcinomas by 10 months of age, male L-JAK2 KO mice in particular showed a remarkable protection against hepatocellular carcinoma and exhibited significantly fewer tumors per liver than littermate controls (Fig. 2, *C* and *D*). JAK2 deficiency also led to a reduction in tumor number per mouse, maximum tumor size per mouse, and overall incidence of tumors (Fig. 2*D*). In line with the lower susceptibility to DEN-induced carcinogenesis in females (24), tumor burden in these mice was markedly lower compared with male counterparts (Fig. 2*E*). Likely as a result of this already low risk, JAK2 deficiency did not have a significant impact on tumor size, multiplicity, or incidence in female mice (Fig. 2*E*). Together, these data suggest that hepatic lipid accumulation *per se* does not promote cancer progression. Indeed, despite development of extensive steatosis, disrupting JAK2 signaling in the liver confers protection from chemical carcinogenesis.

Hepatic JAK2 Deficiency Increases Cell Death and Reduces Cancer Cell Proliferation—Hepatocellular carcinoma occurs on a background of chronic liver injury, which triggers compensatory cellular proliferation and promotes tumor growth (1). To assess whether JAK2 deficiency alters the liver's susceptibility to injury, we examined the acute hepatotoxicity of DEN in L-JAK2 KO mice. To this end, we injected DEN (100 mg/kg) into 8-week-old mice and examined cell turnover 48 or 72 h later. TUNEL assay revealed an increase in hepatocyte death in livers of L-JAK2 KO mice 48 h after DEN challenge (Fig. 3*A*). Furthermore, we observed the presence of TUNEL-positive foci that were not apparent in liver sections from control mice. These results suggest that JAK2 functions to promote hepatocyte survival. Of note, in both genotype groups, DEN at a carcinogenic dose induced cell death in only a small fraction of hepatocytes. Nevertheless, this amount of apoptosis was able to trigger compensatory proliferation of the remaining hepato-

[5] The abbreviations used are: DEN, diethylnitrosamine; MCD, methionine-choline deficient; GH, growth hormone; ROS, reactive oxygen species; TG, triglyceride.

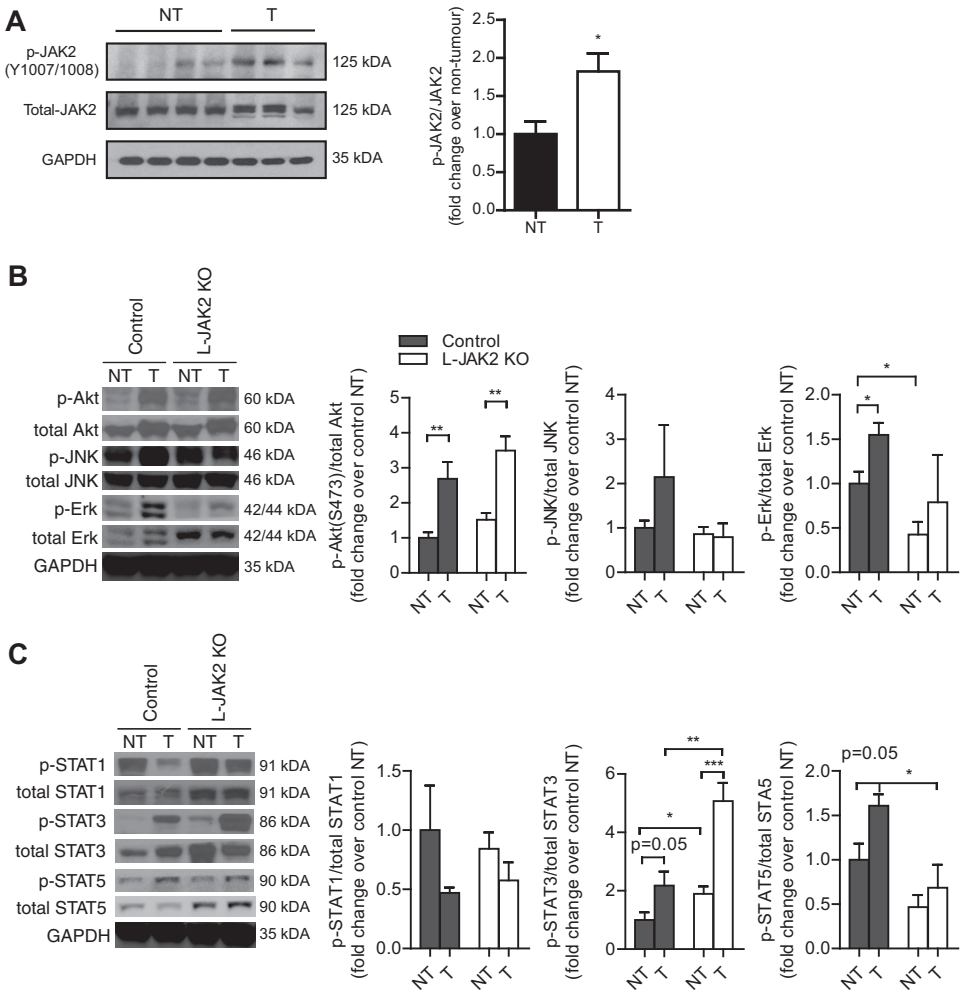

FIGURE 1. **Activation of JAK2 signaling in hepatocellular carcinoma.** Animals were examined at 10 months of age after administration of DEN (25 mg/kg) at 14 days of age. *A*, immunoblot analysis of phospho-JAK2(Y1007/1008) levels in tumor (*T*) and non-tumor (*NT*) tissue from wild-type male mice ($n = 3$). *B* and *C*, immunoblots for p-Akt, p-JNK, and p-Erk (*B*) and p-STAT1, p-STAT3, and p-STAT5 (*C*) in liver tissue from control and L-JAK2 KO mice ($n = 3$). Results are the mean ± S.E. *, $p < 0.05$; **, $p < 0.01$; ***, $p < 0.001$.

cytes due to the liver's high regenerative capacity. Indeed, by Ki67 immunostaining, we observed the presence of proliferating cells 72 h after DEN challenge (Fig. 3*B*). In keeping with the augmented DEN-induced apoptosis, we expected L-JAK2 KO mice to show enhanced compensatory proliferation. Surprisingly, livers from L-JAK2 KO mice exhibited a similar number of proliferating cells in response to DEN compared with control littermates (Fig. 3*B*), suggesting that JAK2 deficiency uncouples liver regeneration from injury.

We next examined liver injury and cell turnover in mice with established hepatocellular carcinomas. At 10 months of age, both genotype groups showed signs of liver damage, as assessed by serum transaminase levels, but there was no significant difference between the groups (Fig. 4*A*). In addition, tumor tissue from both genotype groups up-regulated expression of the pro-fibrogenic factor TGFβ to a similar extent (Fig. 4*B*). Expression of p53 was induced in tumor tissue and so were its effectors Puma and Noxa, but no difference was observed between L-JAK2 KO mice and control littermates (Fig. 4*C*). The pro-apoptotic factors Bak and Bax seemed to be largely unaffected by tumor status or JAK2 disruption, whereas the pro-survival factors Bcl2 and Bcl-xL were up-regulated in tumor tissue but not changed by JAK2 deficiency (Fig. 4*C*). Nevertheless, more foci of TUNEL-positive cells were apparent in liver sections from L-JAK2 KO mice (Fig. 3*C*), similar to the earlier time point examined. In contrast, livers from L-JAK2 KO mice exhibited fewer proliferating cells compared with control littermates (Fig. 3*D*). Furthermore, although expression of cyclin D1 was increased in non-tumor tissue from L-JAK2 KO mice, JAK2 deficiency abolished the induction of cyclin D1 and E expression in tumor tissue (Fig. 3*E*). Thus, the long term effect of JAK2 deficiency on hepatocyte turnover is to increase cell death and reduce cell proliferation. Taken together, these results suggest that JAK2 deficiency alters signaling pathways that regulate hepatocyte proliferation independently of cellular damage.

Hepatic JAK2 Deficiency Reduces Liver Inflammation—To identify signaling molecules responsible for increased hepatocyte death and reduced proliferation, we examined the effect of JAK2 deficiency on several signaling molecules known to modulate hepatocellular carcinoma development. Increased Akt phosphorylation was evident in hepatocellular carcinoma compared with non-tumor tissues, but no difference was observed between the genotype groups (Fig. 1*B*). On the other hand, although development of tumors led to increased Erk and JNK

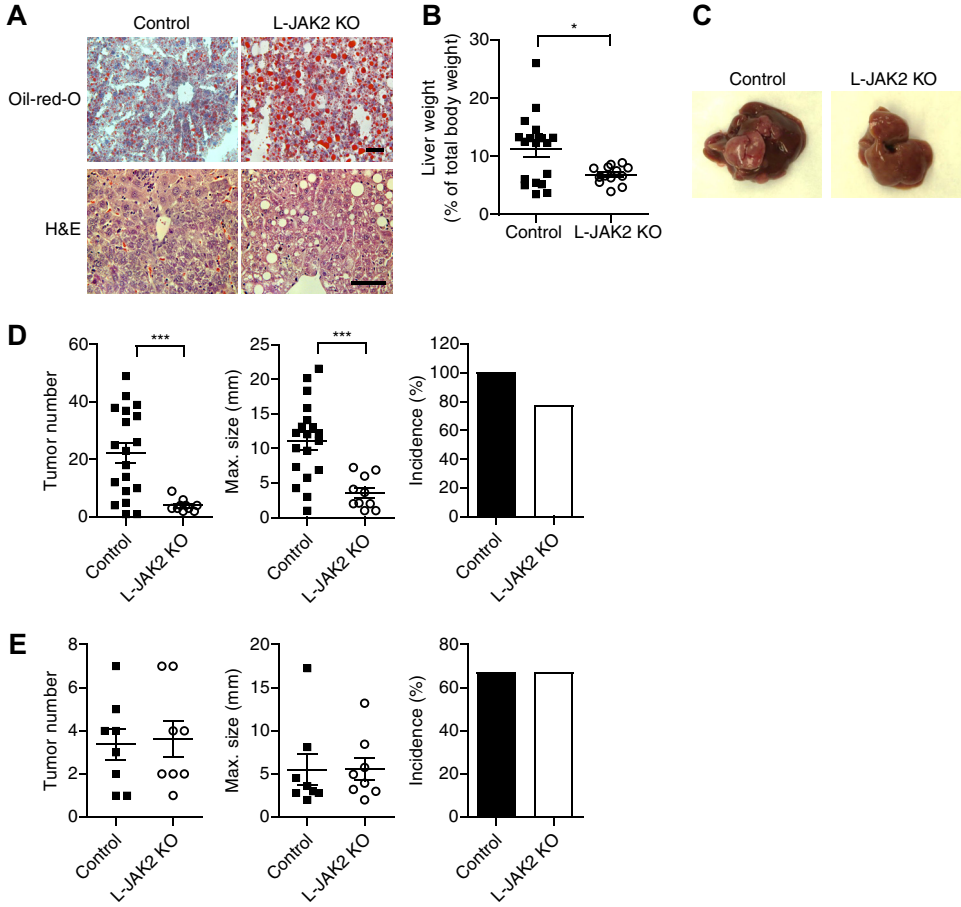

FIGURE 2. **L-JAK2 KO mice are protected from chemically induced liver tumor development.** Animals were examined at 10 months of age after administration of DEN (25 mg/kg) at 14 days of age. *A*, representative micrographs of Oil-red-O and H&E staining of liver sections from animals treated with DEN. *Scale bar*, 50 μm. *B*, liver weight normalized to total body weight in male mice ($n \geq 10$). *C*, representative pictures showing livers of male mice treated with DEN. *D* and *E*, tumor number, size, and incidence in livers of male (*D*) or female (*E*) mice at 10 months of age ($n \geq 10$). Results are the mean ± S.E. *, $p < 0.05$; ***, $p < 0.001$.

phosphorylation in control mice, this increase was largely abolished in L-JAK2 KO mice (Fig. 1*B*). L-JAK2 KO mice also exhibited attenuated Erk phosphorylation in non-tumor tissue compared with control littermates.

Next, we evaluated the impact of JAK2 disruption on the JAK-STAT signaling cascade. Tumor development was associated with attenuated phosphorylation of the anti-tumor transcription factor STAT1, with no significant difference between genotype groups (Fig. 1*C*). In contrast, JAK2 disruption abolished the increase in STAT5 phosphorylation in hepatocellular carcinomas (Fig. 1*C*). STAT3 phosphorylation was also increased in tumor tissue (Fig. 1*C*), consistent with activation of this oncogenic transcription factor. Notably, both non-tumor and tumor tissue from L-JAK2 KO mice exhibited elevated STAT3 phosphorylation compared with control littermates (Fig. 1*C*), which are in line with our previous findings (18) and suggest activation by other kinases. Nevertheless, this increase seemed insufficient for tumor promotion in our model. In fact, although STAT3 phosphorylation was increased in the setting of JAK2 deficiency, we observed reduced hepatic expression of IL-6 (Fig. 5*A*), a STAT3-activating cytokine implicated in tumor promotion (14). There was also a remarkable reduction in circulating IL-6 levels in L-JAK2 KO mice compared with control littermates with no difference in tissue levels by ELISA, suggesting differences were primarily in circulating IL-6 (Fig. 5*B*, supplemental Fig. S3*B*). Similar to IL-6, both tumor and non-tumor tissue from L-JAK2 KO mice exhibited reduced expression of the proinflammatory cytokine IL-1β compared with control mice (Fig. 5*A*). There was no difference in gene expression of IL-6 or IL-1β between tumor and non-tumor tissue within control or L-JAK2 KO groups (Fig. 5*A*). In addition, TNF-α mRNA expression was enhanced only in hepatocellular carcinoma compared with non-tumor tissue from control mice but not in tumor *versus* non-tumor tissue from L-JAK2 KO mice (Fig. 5*A*, supplemental Fig. S3*B*). In line with this, circulating TNF-α concentration was lower in L-JAK2 KO mice (Fig. 5*B*). On the other hand, circulating and gene expression levels of the chemokine MCP-1 were increased in L-JAK2 KO mice compared with control mice (Fig. 5*B*, supplemental Fig. S3*A*). Macrophage F4/80 gene expression was not different between control and L-JAK2 KO mice (supplemental Fig. S3*C*). Female mice showed a similar trend without reaching statistical significance between the genotype groups (supplemental Fig. S3*D*).

Because reactive oxygen species (ROS) have been implicated in hepatocellular carcinoma pathogenesis, we measured thiobarbituric acid-reactive substances (TBARS), a ROS product, which was not changed with JAK2 deficiency (supplemental Fig. S4*A*). The expression of genes involved in endoplasmic reticu-

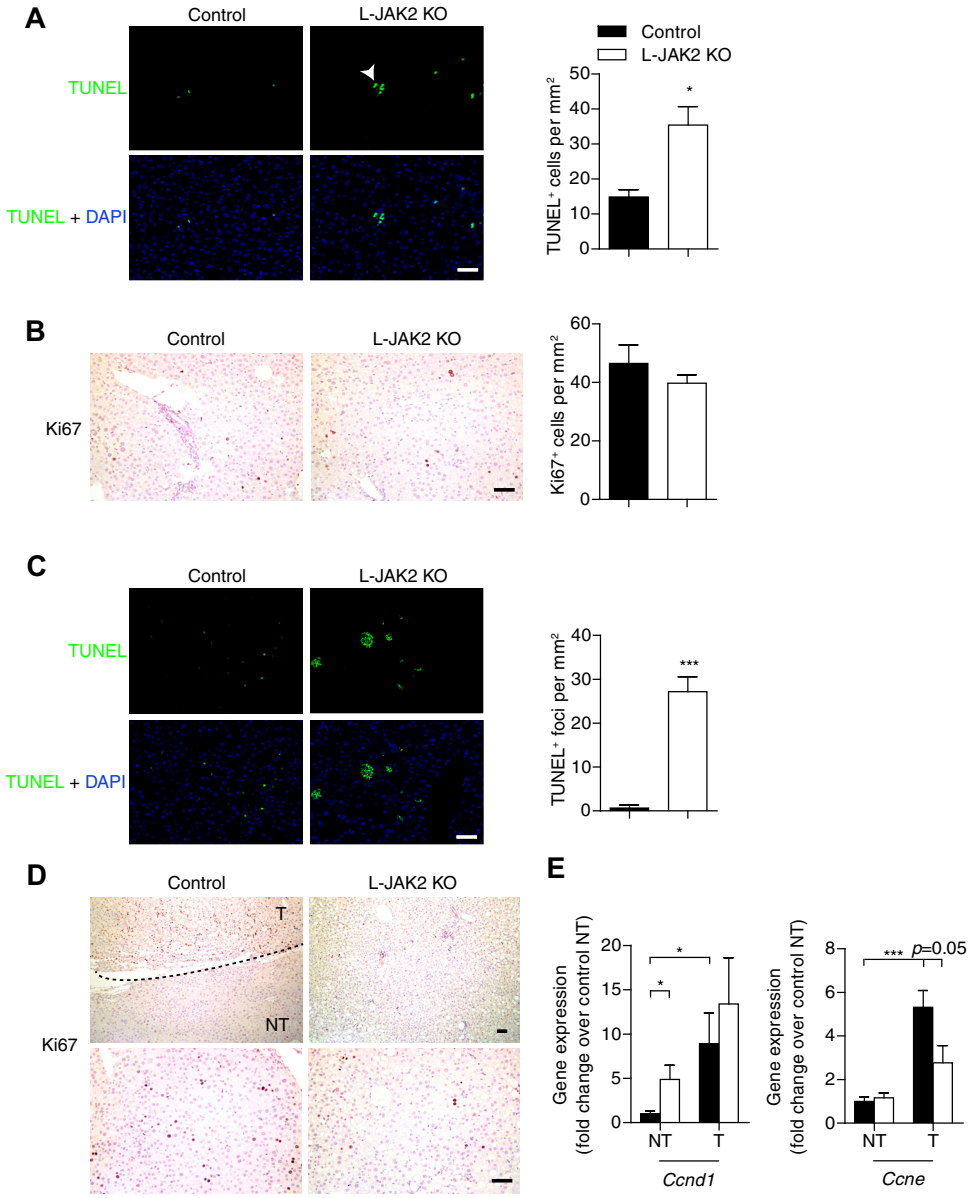

FIGURE 3. **Hepatic JAK2 deficiency increased DEN-induced cell death and reduced cancer cell proliferation.** *A* and *B*, 8-week-old male mice were injected with DEN (100 mg/kg) and sacrificed 48 or 72 h later. *A*, liver sections were stained with TUNEL (*upper panels*) and counterstained with DAPI (*lower panels*). Numbers of TUNEL-positive cells were normalized to area of the section ($n = 4$). *Arrowhead*, dead hepatocyte foci. *B*, Ki67 immunostaining in liver sections. Numbers of Ki67-positive cells were normalized to area of the section ($n \geq 3$). *C–E*, male mice were injected with DEN (25 mg/kg) at 14 days of age and examined at 10 months of age. Shown is TUNEL (*C*) and Ki67 (*D*) immunostaining of liver sections. *Scale bar*, 50 μm. *E*, mRNA expression of genes regulating cell cycle progression ($n = 5$). Results are the mean ± S.E. *, $p < 0.05$; ***, $p < 0.001$. *NT*, non-tumor.

lum stress were increased in L-JAK2 KO mice compared with controls, particularly in non-tumor tissue, consistent with increased cellular injury dissociated from inflammation (supplemental Fig. S4*B*). These data suggest that hepatic JAK2 is not required for the regulation of ROS and dissociates injury from inflammation and hepatocellular carcinoma development in the liver. Together, these results suggest that JAK2 is essential predominantly for the inflammatory response in the liver such that its deficiency attenuates inflammation both locally in the liver and systemically in the circulation.

Hepatic JAK2 Deficiency Protects from MCD Diet-induced Hepatic Lipid Accumulation—Next, to further assess the role of JAK2 in the inflammatory progression of non-alcoholic fatty liver disease and the development of non-alcoholic steatohepatitis, we employed the MCD diet model to induce steatohepatitis. Feeding mice with an MCD diet induces marked intrahepatic lipid accumulation, inflammatory damage, and liver fibrosis. The extent of hepatocyte apoptosis, inflammation, and oxidative stress in this model is greater than that seen in other models of non-alcoholic steatohepatitis (25). L-JAK2 KO mice and control littermates were fed a MCD diet for 8 weeks starting at 2 months of age. In line with reports in the literature (26–28), MCD diet feeding induced an ~50% weight loss in both control and L-JAK2 KO mice (supplemental Fig. S5*A*). Notably, consistent with previous findings (18, 19), L-JAK2 KO mice had lower body weight than littermate controls on both chow and the MCD diet (supplemental Fig. S5*A*). In addition, similar to a high fat diet (18), MCD diet-fed L-JAK2 KO mice

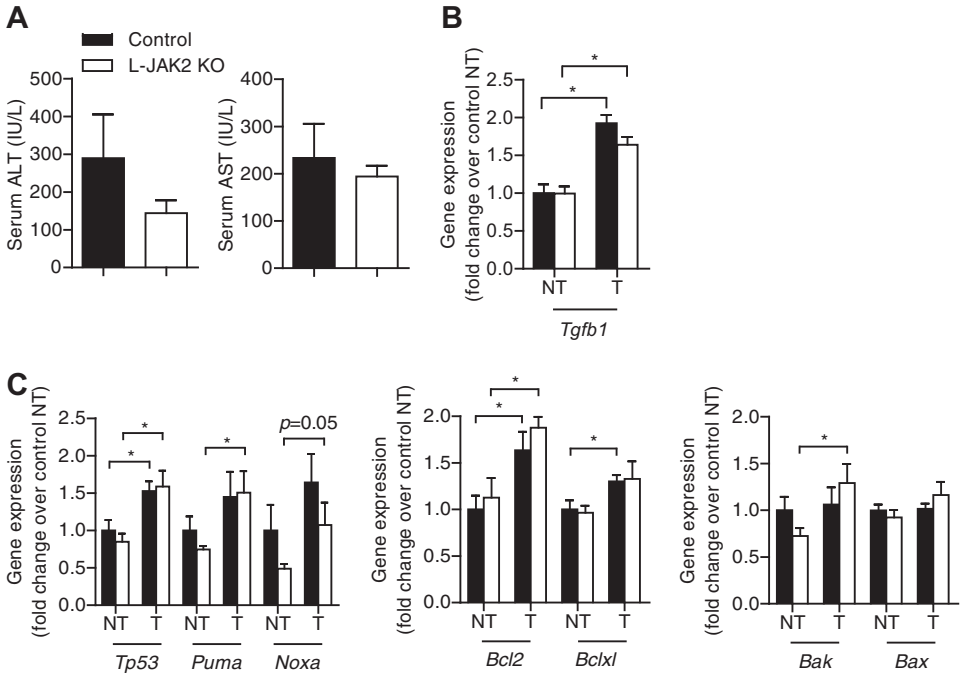

FIGURE 4. **Hepatic JAK2 deficiency in hepatocellular carcinoma-bearing mice increases cell death.** Male mice were injected with DEN (25 mg/kg) at 14 days of age and examined at 10 months of age. *A*, serum alanine aminotransferase (*ALT*) and aspartate aminotransferase (*AST*) levels ($n = 5$). *B* and *C*, mRNA expression of genes regulating fibrogenesis (*B*) and survival and apoptosis (*C*) in tumor (*T*) and non-tumor (*NT*) tissue ($n = 5$). Results are the mean ± S.E. *, $p < 0.05$.

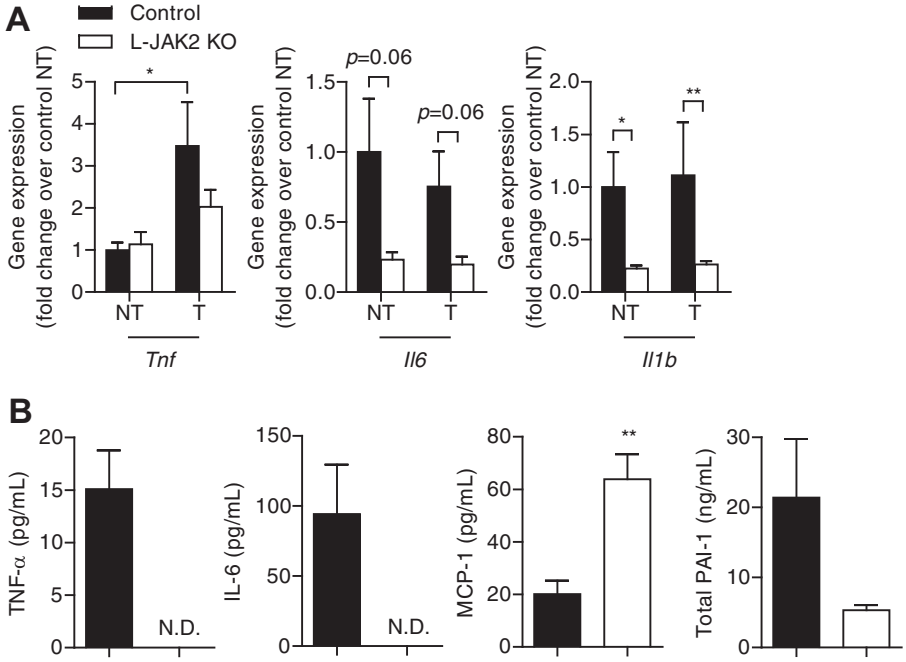

FIGURE 5. **L-JAK2 KO mice show attenuated liver inflammation.** Male mice were injected with DEN (25 mg/kg) at 14 days of age and examined at 10 months of age. *A*, mRNA expression of genes encoding proinflammatory cytokines in male mice ($n = 5$). *B*, serum levels of proinflammatory cytokines in male mice ($n = 5$). N.D., not detected. Results are mean ± S.E. *, $p < 0.05$; **, $p < 0.01$. *T*, tumor; *NT*, non-tumor.

exhibited improved glucose tolerance compared with control littermates (supplemental Fig. S5, *B–D*). On the other hand, insulin sensitivity was not significantly affected by hepatic JAK2 disruption in the setting of MCD (supplemental Fig. S5*E*).

MCD diet feeding led to marked intrahepatic lipid accumulation in control mice, as shown by H&E and Oil-red-O staining as well as biochemical measurements of hepatic triglyceride (TG) levels (Fig. 6, *A–C*). In control mice, despite inducing extensive steatosis, MCD did not significantly affect relative liver weight (Fig. 6*D*). In contrast, although L-JAK2 KO mice developed spontaneous and profound steatosis on chow diet, they did not further accumulate more lipids when placed on an MCD diet (Fig. 6, *A–C*). Indeed, liver tissue from MCD diet-fed L-JAK2 KO mice exhibited lower triglyceride content compared with their control counterparts (Fig. 6*C*). In contrast to triglycerides, hepatic cholesterol content was similar between

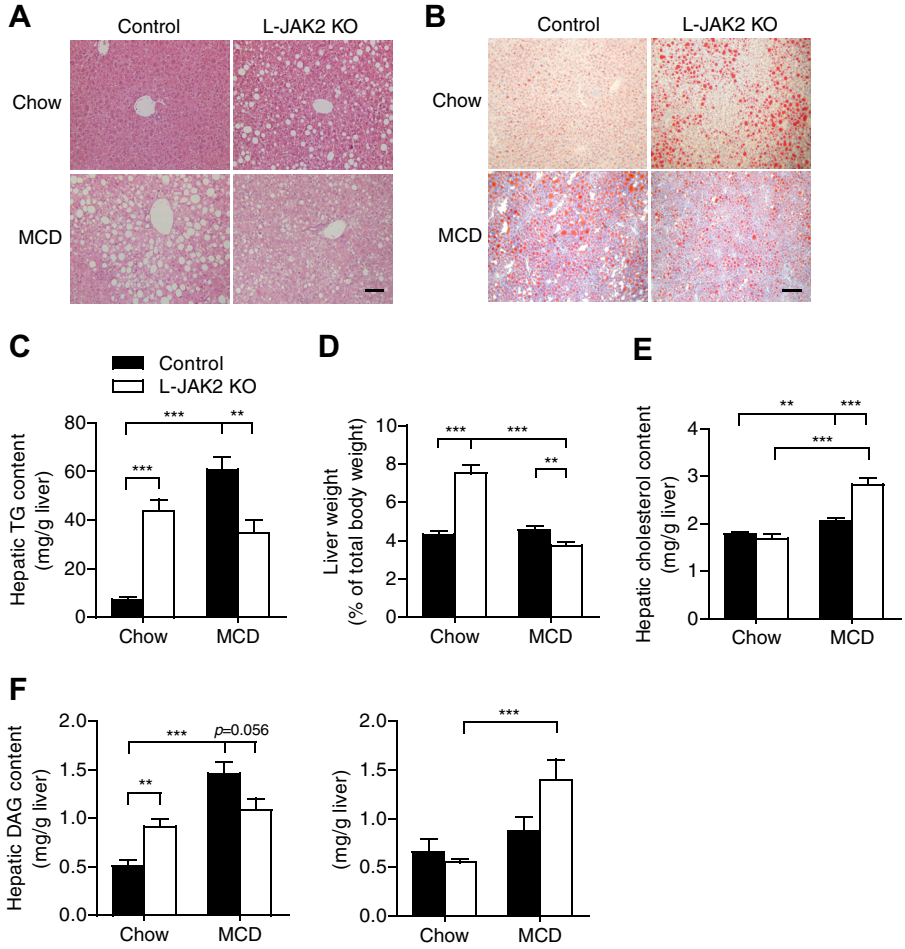

FIGURE 6. **L-JAK2 KO mice are protected from MCD diet-induced hepatic lipid accumulation.** *A*, representative micrographs of H&E staining of liver sections from mice fed a standard chow or MCD diet for 8 weeks starting at 8 weeks of age. *Scale bar*, 50 μm. *B*, representative micrographs of Oil-red-O staining of liver sections. Lipid appears *bright red*. *Scale bar*, 100 μm. *C*, hepatic TG content normalized to tissue weight ($n \geq 4$). *D*, liver weight normalized to total body weight ($n \geq 13$). *E*, hepatic cholesterol content ($n \geq 4$). *F*, hepatic diacylglycerol (*DAG*) and free fatty acid (*FFA*) content ($n \geq 4$). Results are mean ± S.E. **, $p < 0.01$; ***, $p < 0.001$.

the two genotype groups on the chow diet (Fig. 6*E*). After MCD feeding, a small but significant increase in cholesterol levels was observed in control mice, and this increase was more profound in L-JAK2 KO mice (Fig. 6*E*). We also analyzed levels of lipid metabolites in the liver in response to MCD diet feeding. Diacylglycerol followed a similar trend as TG, with MCD diet elevating its levels in control but not L-JAK2 KO mice (Fig. 6*F*). Interestingly, free fatty acid levels did not change in control mice but were significantly elevated in L-JAK2 KO mice following MCD diet feeding (Fig. 6*F*). Taken together, these data suggest that JAK2 is required for MCD diet-induced hepatic steatosis.

Hepatic JAK2 Deficiency Arrests the Development of MCD Diet-induced Steatohepatitis—We next examined the effect of hepatic JAK2 disruption on MCD-induced steatohepatitis. Under basal chow-fed conditions, livers of L-JAK2 KO mice showed increased mRNA expression of the proinflammatory cytokine TNF-α (Fig. 7*A*). In contrast, hepatic expression of the proinflammatory cytokines IL-6, IL-1β, and IFNγ was attenuated by JAK2 disruption (Fig. 7*A*). Upon MCD diet feeding, TNF-α expression was up-regulated in both genotype groups but with a blunted induction in L-JAK2 KO mice. On the other hand, expression of IL-6, IL-1β, and IFNγ was down-regulated in both genotype groups (Fig. 7*A*).

Liver fibrosis develops as a result of chronic liver injury and can subsequently increase hepatocellular carcinoma risk. Levels of cell death were increased to a similar extent in both control and L-JAK2 KO mice, as shown by TUNEL and immunostaining for cleaved caspase 3 (supplemental Fig. S6). We, therefore, assessed fibrosis by measuring hepatic expression of markers of fibrosis. As shown in Fig. 7*B*, MCD diet feeding up-regulated expression of pro-collagen 1α and α-smooth muscle actin in control mice, suggesting activation of a profibrogenic response. Interestingly, livers of L-JAK2 KO mice showed similar or higher expression of these genes under basal conditions, but MCD diet feeding did not elevate their expression further (Fig. 7*B*). By Masson's trichrome stain, we observed development of portal fibrosis in both genotype groups (Fig. 7*C*). Taken together, these data suggest that development of MCD diet-induced steatohepatitis occurs to a lesser extent in the setting of JAK2 deficiency.

Discussion

The prevalence of hepatocellular carcinoma is expected to rise dramatically due to the growing epidemic of non-alcoholic fatty liver disease worldwide. Although cirrhosis remains the leading risk factor for hepatocellular carcinoma, a significant

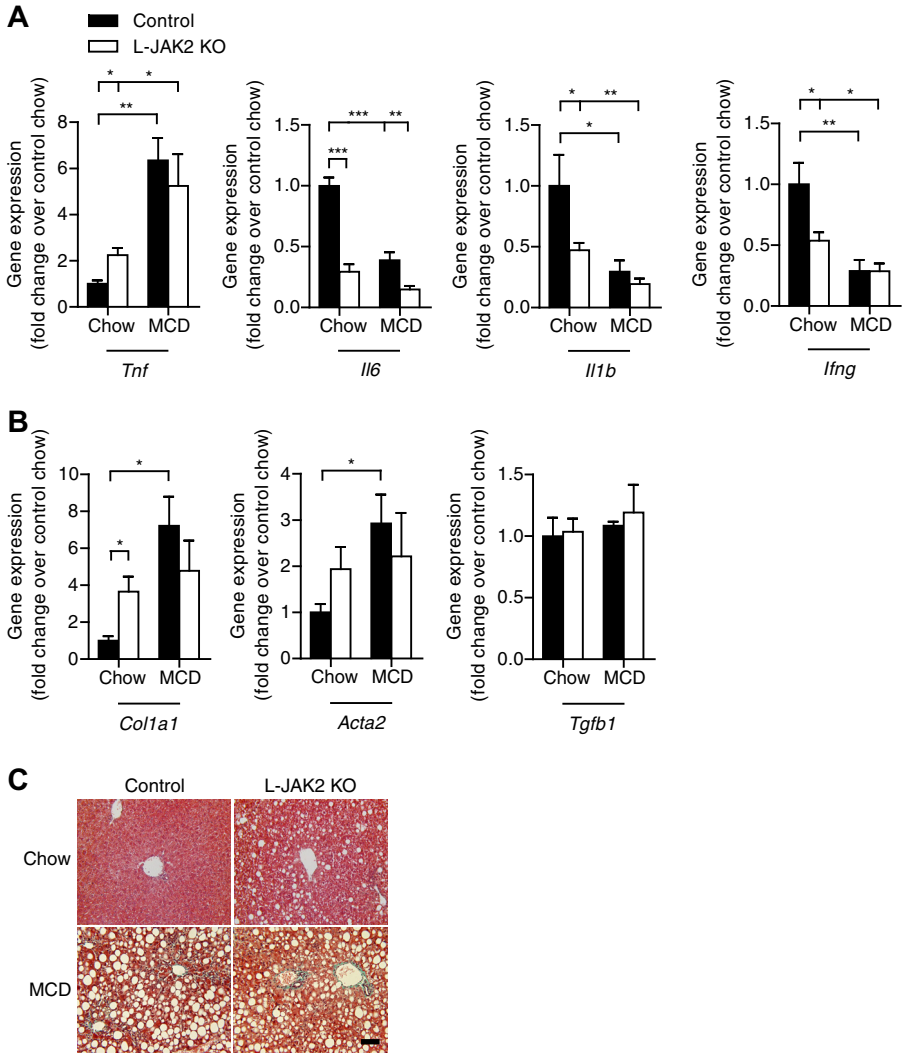

FIGURE 7. **MCD-induced steatohepatitis development is arrested in L-JAK2 KO mice.** *A* and *B*, mRNA expression of genes encoding proinflammatory cytokines (*A*) and pro-fibrogenic factors (*B*) ($n \geq 4$). *C*, representative micrographs of Masson's trichrome staining of liver sections. *Scale bar*, 50 μm. Results are the mean ± S.E. *, $p < 0.05$; **, $p < 0.01$; ***, $p < 0.001$.

proportion of non-alcoholic steatohepatitis-associated hepatocellular carcinoma cases occur in the absence of apparent cirrhosis (29). Thus, whether hepatosteatosis *per se* can promote hepatocarcinogenesis is not well understood. Using models of both hepatosteatosis and hepatocarcinogenesis, we now demonstrate that isolated steatosis in the setting of hepatic JAK2 disruption was insufficient for accelerating chemically induced liver tumor development. Rather, JAK2 appears to be essential for inflammation, and we show this to be a requisite process for tumorigenesis. As such, hepatic JAK2 deficiency provides a profound protection against hepatocellular carcinoma (supplemental Fig. S7).

Hepatocellular carcinoma represents a classic case of inflammation-linked cancer. In addition to hepatocellular carcinoma, other malignancies whose development is linked to chronic inflammation include cancer of the lungs, bladder, and the gastrointestinal tract (30). In these cancer types, inhibition of JAK2 signaling has been shown to suppress tumor cell growth (31–33), indicating that JAK2 has a fundamental role in mediating the link between inflammation and tumorigenesis.

Hepatic JAK2 deficiency disrupts the GH-STAT5-IGF-1 signaling pathway in the liver, leading to significantly attenuated circulating IGF-1 levels. Inhibition of IGF-1 using antisense oligonucleotides has previously been shown to reduce hepatocellular carcinoma growth rates *in vitro* and *in vivo* (34, 35). Given the well known role of IGF-1 as a mitogen, it is not unreasonable to speculate that reduced IGF-1 signaling underlies tumor protection in the setting of hepatic JAK2 deficiency. Nevertheless, previous studies have shown that hepatocyte-specific deletion of STAT5, which also abolishes IGF-1 secretion, actually accelerated carbon tetrachloride-induced liver cancer development (36). Therefore, impaired IGF-1 signal transduction seems unlikely to be the major anti-tumor mechanism in L-JAK2 KO mice. Nevertheless, further work is required to determine the role of IGF-1 attenuation in the prevention of hepatocellular carcinoma development in this setting.

Intriguingly, hepatic JAK2 disruption was associated with increased hepatocellular death both as an acute response to DEN and at later stages of cancer development. Pending further investigation, this may be due to the loss of signaling of hepa-

toprotective factors as a result of JAK2 deficiency. Notably, STAT5, whose activity was moderately reduced in JAK2-deficient liver tissue, promotes transcription of known hepatoprotective genes including leukemia inhibitory factor receptor, prolactin receptor, epithelial growth factor receptor, and hepatocyte nuclear factor 6 (37). Furthermore, ligands for these receptors, in particular prolactin and leukemic inhibitor factor, signal through JAK2.

It is proposed that hepatocyte death after cellular injury activates adjacent immune cells in the liver, such as resident macrophages (Kupffer cells) (11), CD8+ T cells, and NKT cells (38). These immune cells in turn produce hepatomitogens that enhance compensatory proliferation of surviving hepatocytes (39). In our model of hepatic JAK2 deficiency, cell death and endoplasmic reticulum stress were increased, whereas ROS levels were unchanged, and inflammation and regeneration was attenuated. Uncoupling of hepatocellular death and compensatory proliferation with loss of JAK2 specifically in hepatocytes suggests that two mechanisms could be at play. Namely, either the stress signal released by dead hepatocytes is defective or secreted hepatomitogens could not activate cellular proliferation pathways in hepatocytes. Of note, hepatic expression of the liver growth factors TNF-α and IL-6 was reduced in L-JAK2 KO mice, suggesting that activation of hepatic immune cells is impaired (11). With an MCD diet-induced model of steatohepatitis, disruption of JAK2 resulted in a smaller increase in TNFα and decreased IL-6, IL-1b, and IFNγ in the liver. These findings are consistent with disruption of JAK2 resulting in decreased inflammation in the setting of steatosis.

In particular, IL-6 is a prominent tumor-promoting cytokine that functions downstream of both TNF-α and IL-1 (40). Mice lacking IL-6 exhibit lower tumor burden compared with wild-type mice when challenged with DEN (24). IL-6 is also hepatoprotective and required for normal liver regeneration (41). Therefore, attenuated IL-6 signaling may contribute to cancer protection in L-JAK2 KO mice. Of note, canonical IL-6 signaling is mediated by the JAK2-STAT3 pathway (42). Surprisingly, STAT3 activity was increased in JAK2-deficient liver tissue despite lower IL-6 levels. These results suggest that the tumor-promoting effect of IL-6 may be mediated, at least in part, via STAT3-independent mechanisms. Indeed, IL-6 also signals through Erk (40) and along with IL-6 expression, Erk activation was attenuated in JAK2-deficient liver tissue.

In addition to regulating cell death and proliferation, JAK2 may also play a role in later stages of hepatocarcinogenesis. It was previously shown that JAK2 expression positively correlates with portal hypertension and decompensation in human cirrhosis. In animal models, treatment with AG490, a JAK2 inhibitor, decreased hepatic vascular resistance and portal pressure associated with liver cirrhosis *in vivo* and *in situ* (43), suggesting a permissive role of JAK2 in end-stage progression of steatohepatitis. In our model, development of fibrosis occurred to a similar extent in MCD diet-fed L-JAK2 KO mice and control littermates, suggesting that JAK2 does not play a direct role in fibrogenesis.

Interestingly, cancer protection was not observed in female L-JAK2 KO mice, as they exhibited a similar tumor burden as control littermates. This may be due to the much lower cancer risk in females compared with male counterparts, thus requiring a much larger sample number for definitive conclusions (44). Of note, female mice have been shown to produce significantly less IL-6 in response to DEN (24), and our results are in keeping with this notion. Therefore, although JAK2 disruption leads to greatly attenuated IL-6 levels in male mice, the reduction in IL-6 in female mice may not be significant enough to translate into detectable changes in cancer risk.

In summary, our results show that loss of JAK2 in hepatocytes impairs inflammatory activation in response to chemical carcinogen challenge. Accordingly, although L-JAK2 KO mice were susceptible to DEN-induced hepatocellular death, this was not accompanied by compensatory proliferation. Consequently, L-JAK2 KO mice were remarkably protected from liver cancer development. Taken together, our work uncovers an indispensable role of JAK2-mediated inflammatory signaling in the pathogenesis of hepatocellular carcinoma. Targeting the JAK-STAT pathway may provide a novel therapeutic strategy for the treatment of this deadly disease.

Experimental Procedures

Animal Model—Mice with hepatocyte-specific JAK2 deficiency (herein referred to as L-JAK2 KO mice) driven by the *Albumin* promoter were described previously (18). *Albumin* $Cre^{+}Jak2^{+/+}$ littermates served as controls in this study, and both male and female mice were used. Animals were housed in a temperature-controlled and pathogen-free facility at the Toronto Medical Discovery Tower (Toronto, ON, Canada) with a 12-h light-dark cycle and free access to water and standard irradiated rodent chow. All animal experimental protocols were approved by the Toronto General Hospital Research Institute Animal Care Committee.

Tumor Induction and Analysis—Fourteen-day-old mice were injected i.p. with 25 mg/kg DEN (Sigma) dissolved in 0.9% NaCl. After 10 months, all mice were sacrificed. Their livers were removed and separated into individual lobes. Grossly visible tumors ($\geq$0.5 mm) in each lobe were counted, and their size was measured. Lobes were microdissected into tumor and non-tumor tissue and stored at −80 °C until analyzed. To assess the acute toxicity of DEN, 8-week-old mice were injected i.p. with 100 mg/kg DEN. Mice were sacrificed 48 or 72 h later for analysis.

MCD Diet Feeding—Starting at 8 weeks of age, L-JAK2 KO and control littermates were fed either a control chow diet or a diet completely devoid of methionine and choline (D518810; Dyets Inc., Bethlehem, PA) for 8 weeks. Body weight was measured weekly on the assigned diets.

In Vivo Metabolic Analyses—In vivo metabolic analyses were performed as previously described (45, 46). Briefly, glucose tolerance tests were performed on animals fasted overnight for 14–16 h at an i.p. injection dose of 1 g/kg body weight. Insulin tolerance tests were performed on randomly fed animals using human regular insulin (Humulin R, Lilly) at an i.p. injection dose of 0.5 unit/kg body weight. For both glucose tolerance and insulin tolerance tests, blood glucose levels were measured from tail veins using a glucometer (FreeStyle Lite, Abbott Diabetes Care Inc., Alameda).

Analysis of Serum Parameters—Blood was collected by cardiac puncture into serum separator tubes and centrifuged at 5000 × *g* for 10 min. Circulating TNF-α, IL-6, and MCP-1 were determined by the Milliplex mouse serum adipokine kit (Millipore, Billerica, MA). Serum alanine aminotransferase and aspartate aminotransferase levels were measured by IDEXX Ltd. (Markham, Ontario, Canada). Serum GH and IGF-1 levels were determined by radioimmunoassay at the Mouse Metabolic Phenotyping Centre (Vanderbilt University, Nashville, TN).

Lipid Content—Total lipids from liver were extracted by the Folch technique and separated by thin-layer chromatography. Fatty acids were collected, hydrolyzed, converted to fatty acid methyl esters using 14% boron trifluoride-methanol, and then quantified using a Varian-430 gas chromatograph (Varian, Lake Forest, CA) equipped with a flame-ionization detector. The concentration of each fatty acid at baseline was calculated via comparison to the internal control heptadecanoic acid (17:0) made at known concentrations. Cholesterol levels were measured by gas chromatography-mass spectrometry. Briefly, extracted total lipids were spiked with 5α-cholestane as an internal standard. The mixture was saponified with NaOH-methanol, and hexane was added to separate non-saponifiable cholesterol from saponified fatty acids. The hexane fraction containing the cholesterol was then extracted, and trimethylsilyl chloride was added to derivatize for analysis by an Agilent 6890 gas chromatograph with an Agilent 5973 Network Mass Selective Detector (47).

Histology, Immunohistochemistry, and Immunofluorescent Staining—Liver tissues were harvested, fixed in 4% paraformaldehyde in 0.1 M PBS (pH 7.4), and processed to paraffin blocks. Slides were cut in 7-μm sections with a 150-μm separation on three levels and stained with H&E, Masson's trichrome stain, TUNEL (Roche Applied Science) and immunohistochemical staining for Ki67 (DAKO, Glostrup, Denmark). Immunofluorescent images were obtained by a Zeiss inverted fluorescent microscope (Advanced Optical Microscopy Facility, Toronto, Ontario, Canada). TUNEL and Ki67-positive cells were counted and normalized to area of the liver section. For Oil-red-O staining, liver tissues were harvested, embedded in Tissue-Tek® O.C.T. compound (Sakura Finetek, Torrance, CA), and snap-frozen. Frozen specimens were cut in 10-μm sections and stained with Oil-red-O to visualize neutral lipids.

RNA Isolation and Quantitative RT-PCR—Total RNA from liver tissues was isolated using the TRIzol reagent (Invitrogen). RNA was reverse-transcribed to cDNA with random primers using the M-MLV enzyme (Invitrogen). Quantitative RT-PCR was performed using specific primers and SYBR Green master mix (Applied Biosystems, Carlsbad, CA) on a 7900HT Fast-Real-Time PCR System (Applied Biosystems). Each sample was run in triplicate. The relative mRNA abundance of each gene was normalized to the expression levels of the housekeeping gene *18s*.

Immunoblotting—Liver tissues were mechanically homogenized in ice-cold lysis buffer and centrifuged at 14,000 × *g* for 10 min at 4 °C. The resulting supernatant was separated by SDS-PAGE and immunoblotted with antibodies to JAK2, Akt, STAT1, STAT3, STAT5, GAPDH (Cell Signaling Technology, Danvers, MA), JNK, and Erk (Santa Cruz Biotechnology). Protein band intensity was quantified by ImageJ software.

ROS Measurement—25 mg of liver tissue was homogenized in 250 μl of radioimmune precipitation assay buffer with 1:1000 protease inhibitor. ROS was measured using a thiobarbituric acid-reactive substances kit (TBARS kit; Cayman Chemical) as per the manufacturer's instructions.

Statistical Analysis—Data are presented as the means ± S.E. of the mean. Values were analyzed by two-tailed independent-sample Student's *t* test or one-way analysis of variance followed by Tukey's post-tests, as appropriate, using GraphPad Prism version 5 (GraphPad Software, La Jolla, CA). p values < 0.05 were considered as statistically significant.

Author Contributions—S. Y. S. and M. W. designed the study and wrote the paper. S. Y. S., C. T. L., S. A. S., M. J. K., D. W. D., T. S., L. L., S.-Y. L., and E. P. C. performed the experiments and acquired the data. K.-U. W. generated the Jak2 floxed mice. R. P. B. provided critical intellectual input. All authors approved the final version of the manuscript.

Acknowledgment—We thank Dr. Oyedele Adeyi (Toronto General Hospital Research Institute) for insightful advice.

References

1. El-Serag, H. B., and Rudolph, K. L. (2007) Hepatocellular carcinoma: epidemiology and molecular carcinogenesis. *Gastroenterology* **132,** 2557–2576
2. Bacon, B. R., Farahvash, M. J., Janney, C. G., and Neuschwander-Tetri, B. A. (1994) Nonalcoholic steatohepatitis: an expanded clinical entity. *Gastroenterology* **107,** 1103–1109
3. Diehl, A. M., Goodman, Z., and Ishak, K. G. (1988) Alcohol-like liver disease in nonalcoholics: a clinical and histologic comparison with alcohol-induced liver injury. *Gastroenterology* **95,** 1056–1062
4. Starley, B. Q., Calcagno, C. J., and Harrison, S. A. (2010) Nonalcoholic fatty liver disease and hepatocellular carcinoma: a weighty connection. *Hepatology* **51,** 1820–1832
5. Poonawala, A., Nair, S. P., and Thuluvath, P. J. (2000) Prevalence of obesity and diabetes in patients with cryptogenic cirrhosis: a case-control study. *Hepatology* **32,** 689–692
6. Day, C. P., and James, O. F. (1998) Steatohepatitis: a tale of two "hits"? *Gastroenterology* **114,** 842–845
7. Nakagawa, H., Umemura, A., Taniguchi, K., Font-Burgada, J., Dhar, D., Ogata, H., Zhong, Z., Valasek, M. A., Seki, E., Hidalgo, J., Koike, K., Kaufman, R. J., and Karin, M. (2014) ER stress cooperates with hypernutrition to trigger TNF-dependent spontaneous HCC development. *Cancer Cell* **26,** 331–343
8. Marra, F., Gastaldelli, A., Svegliati Baroni, G., Tell, G., and Tiribelli, C. (2008) Molecular basis and mechanisms of progression of non-alcoholic steatohepatitis. *Trends Mol. Med.* **14,** 72–81
9. Wree, A., Broderick, L., Canbay, A., Hoffman, H. M., and Feldstein, A. E. (2013) From NAFLD to NASH to cirrhosis-new insights into disease mechanisms. *Nat. Rev. Gastroenterol. Hepatol.* **10,** 627–636
10. Rock, K. L., and Kono, H. (2008) The inflammatory response to cell death. *Annu Rev Pathol* **3,** 99–126
11. Maeda, S., Kamata, H., Luo, J. L., Leffert, H., and Karin, M. (2005) IKKβ couples hepatocyte death to cytokine-driven compensatory proliferation that promotes chemical hepatocarcinogenesis. *Cell* **121,** 977–990
12. Pikarsky, E., Porat, R. M., Stein, I., Abramovitch, R., Amit, S., Kasem, S., Gutkovich-Pyest, E., Urieli-Shoval, S., Galun, E., and Ben-Neriah, Y. (2004) NF-κB functions as a tumour promoter in inflammation-associated cancer. *Nature* **431,** 461–466
13. Sakurai, T., Maeda, S., Chang, L., and Karin, M. (2006) Loss of hepatic NF-κB activity enhances chemical hepatocarcinogenesis through sustained c-Jun N-terminal kinase 1 activation. *Proc. Natl. Acad. Sci. U.S.A.* **103,** 10544–10551

14. Park, E. J., Lee, J. H., Yu, G. Y., He, G., Ali, S. R., Holzer, R. G., Osterreicher, C. H., Takahashi, H., and Karin, M. (2010) Dietary and genetic obesity promote liver inflammation and tumorigenesis by enhancing IL-6 and TNF expression. *Cell* **140,** 197–208
15. Gao, B. (2005) Cytokines, STATs and liver disease. *Cell. Mol. Immunol.* **2,** 92–100
16. Freitas, M. C., Uchida, Y., Zhao, D., Ke, B., Busuttil, R. W., and Kupiec-Weglinski, J. W. (2010) Blockade of Janus kinase-2 signaling ameliorates mouse liver damage due to ischemia and reperfusion. *Liver Transpl.* **16,** 600–610
17. Yu, H., Pardoll, D., and Jove, R. (2009) STATs in cancer inflammation and immunity: a leading role for STAT3. *Nat. Rev. Cancer* **9,** 798–809
18. Shi, S. Y., Martin, R. G., Duncan, R. E., Choi, D., Lu, S. Y., Schroer, S. A., Cai, E. P., Luk, C. T., Hopperton, K. E., Domenichiello, A. F., Tang, C., Naples, M., Dekker, M. J., Giacca, A., *et al.* (2012) Hepatocyte-specific deletion of Janus kinase 2 (JAK2) protects against diet-induced steatohepatitis and glucose intolerance. *J. Biol. Chem.* **287,** 10277–10288
19. Sos, B. C., Harris, C., Nordstrom, S. M., Tran, J. L., Balázs, M., Caplazi, P., Febbraio, M., Applegate, M. A., Wagner, K. U., and Weiss, E. J. (2011) Abrogation of growth hormone secretion rescues fatty liver in mice with hepatocyte-specific deletion of JAK2 . *J. Clin. Invest.* **121,** 1412–1423
20. Anstee, Q. M., and Goldin, R. D. (2006) Mouse models in non-alcoholic fatty liver disease and steatohepatitis research. *Int. J. Exp. Pathol.* **87,** 1–16
21. Schattenberg, J. M., and Galle, P. R. (2010) Animal models of non-alcoholic steatohepatitis: of mice and man. *Dig. Dis.* **28,** 247–254
22. Vesselinovitch, S. D., and Mihailovich, N. (1983) Kinetics of diethylnitrosamine hepatocarcinogenesis in the infant mouse. *Cancer Res.* **43,** 4253–4259
23. Lee, J. S., Chu, I. S., Mikaelyan, A., Calvisi, D. F., Heo, J., Reddy, J. K., and Thorgeirsson, S. S. (2004) Application of comparative functional genomics to identify best-fit mouse models to study human cancer. *Nat. Genet.* **36,** 1306–1311
24. Naugler, W. E., Sakurai, T., Kim, S., Maeda, S., Kim, K., Elsharkawy, A. M., and Karin, M. (2007) Gender disparity in liver cancer due to sex differences in MyD88-dependent IL-6 production. *Science* **317,** 121–124
25. Gao, D., Wei, C., Chen, L., Huang, J., Yang, S., and Diehl, A. M. (2004) Oxidative DNA damage and DNA repair enzyme expression are inversely related in murine models of fatty liver disease. *Am. J. Physiol. Gastrointest. Liver Physiol.* **287,** G1070–G1077
26. Leclercq, I. A., Farrell, G. C., Field, J., Bell, D. R., Gonzalez, F. J., and Robertson, G. R. (2000) CYP2E1 and CYP4A as microsomal catalysts of lipid peroxides in murine nonalcoholic steatohepatitis. *J. Clin. Invest.* **105,** 1067–1075
27. Rinella, M. E., Elias, M. S., Smolak, R. R., Fu, T., Borensztajn, J., and Green, R. M. (2008) Mechanisms of hepatic steatosis in mice fed a lipogenic methionine choline-deficient diet. *J. Lipid Res.* **49,** 1068–1076
28. Weltman, M. D., Farrell, G. C., and Liddle, C. (1996) Increased hepatocyte CYP2E1 expression in a rat nutritional model of hepatic steatosis with inflammation. *Gastroenterology* **111,** 1645–1653
29. Ertle, J., Dechêne, A., Sowa, J. P., Penndorf, V., Herzer, K., Kaiser, G., Schlaak, J. F., Gerken, G., Syn, W. K., and Canbay, A. (2011) Non-alcoholic fatty liver disease progresses to hepatocellular carcinoma in the absence of apparent cirrhosis. *Int. J. Cancer* **128,** 2436–2443
30. Karin, M., and Greten, F. R. (2005) NF-κB: linking inflammation and immunity to cancer development and progression. *Nat. Rev. Immunol.* **5,** 749–759
31. Joung, Y. H., Na, Y. M., Yoo, Y. B., Darvin, P., Sp, N., Kang, D. Y., Kim, S. Y., Kim, H. S., Choi, Y. H., Lee, H. K., Park, K. D., Cho, B. W., Kim, H. S., Park, J. H., and Yang, Y. M. (2014) Combination of AG490, a Jak2 inhibitor, and methylsulfonylmethane synergistically suppresses bladder tumor growth via the Jak2/STAT3 pathway. *Int. J. Oncol.* **44,** 883–895
32. Lee, J. H., Park, K. S., Alberobello, A. T., Kallakury, B., Weng, M. T., Wang, Y., and Giaccone, G. (2013) The Janus kinases inhibitor AZD1480 attenuates growth of small cell lung cancers *in vitro* and *in vivo*. *Clin. Cancer Res.* **19,** 6777–6786
33. Judd, L. M., Menheniott, T. R., Ling, H., Jackson, C. B., Howlett, M., Kalantzis, A., Priebe, W., and Giraud, A. S. (2014) Inhibition of the JAK2/STAT3 pathway reduces gastric cancer growth *in vitro* and *in vivo*. *PLoS ONE* **9,** e95993
34. Ellouk-Achard, S., Djenabi, S., De Oliveira, G. A., Desauty, G., Duc, H. T., Zohair, M., Trojan, J., Claude, J. R., Sarasin, A., and Lafarge-Frayssinet, C. (1998) Induction of apoptosis in rat hepatocarcinoma cells by expression of IGF-I antisense c-DNA. *J. Hepatol.* **29,** 807–818
35. Upegui-Gonzalez, L. C., Duc, H. T., Buisson, Y., Arborio, M., Lafarge-Frayssinet, C., Jasmin, C., Guo, Y., and Trojan, J. (1998) Use of the IGF-I antisense strategy in the treatment of the hepatocarcinoma. *Adv. Exp. Med. Biol.* **451,** 35–42
36. Hosui, A., Kimura, A., Yamaji, D., Zhu, B. M., Na, R., and Hennighausen, L. (2009) Loss of STAT5 causes liver fibrosis and cancer development through increased TGF-β and STAT3 activation. *J. Exp. Med.* **206,** 819–831
37. Yu, J. H., Zhu, B. M., Riedlinger, G., Kang, K., and Hennighausen, L. (2012) The liver-specific tumor suppressor STAT5 controls expression of the reactive oxygen species-generating enzyme NOX4 and the proapoptotic proteins PUMA and BIM in mice. *Hepatology* **56,** 2375–2386
38. Wolf, M. J., Adili, A., Piotrowitz, K., Abdullah, Z., Boege, Y., Stemmer, K., Ringelhan, M., Simonavicius, N., Egger, M., Wohlleber, D., Lorentzen, A., Einer, C., Schulz, S., Clavel, T., Protzer, U., *et al.* (2014) Metabolic activation of intrahepatic CD8+ T cells and NKT cells causes nonalcoholic steatohepatitis and liver cancer via cross-talk with hepatocytes. *Cancer Cell* **26,** 549–564
39. Fausto, N. (2000) Liver regeneration. *J. Hepatol.* **32,** 19–31
40. Kamimura, D., Ishihara, K., and Hirano, T. (2003) IL-6 signal transduction and its physiological roles: the signal orchestration model. *Rev. Physiol. Biochem. Pharmacol.* **149,** 1–38
41. Cressman, D. E., Greenbaum, L. E., DeAngelis, R. A., Ciliberto, G., Furth, E. E., Poli, V., and Taub, R. (1996) Liver failure and defective hepatocyte regeneration in interleukin-6-deficient mice. *Science* **274,** 1379–1383
42. Hodge, D. R., Hurt, E. M., and Farrar, W. L. (2005) The role of IL-6 and STAT3 in inflammation and cancer. *Eur. J. Cancer* **41,** 2502–2512
43. Klein, S., Rick, J., Lehmann, J., Schierwagen, R., Schierwagen, I. G., Verbeke, L., Hittatiya, K., Uschner, F. E., Manekeller, S., Strassburg, C. P., Wagner, K. U., Sayeski, P. P., Wolf, D., Laleman, W., Sauerbruch, T., and Trebicka, J. (2017) Janus-kinase-2 relates directly to portal hypertension and to complications in rodent and human cirrhosis. *Gut* **66,** 145–155
44. Ghebranious, N., and Sell, S. (1998) Hepatitis B injury, male gender, aflatoxin, and p53 expression each contribute to hepatocarcinogenesis in transgenic mice. *Hepatology* **27,** 383–391
45. Wang, L., Opland, D., Tsai, S., Luk, C. T., Schroer, S. A., Allison, M. B., Elia, A. J., Furlonger, C., Suzuki, A., Paige, C. J., Mak, T. W., Winer, D. A., Myers, M. G., Jr, and Woo, M. (2014) Pten deletion in RIP-Cre neurons protects against type 2 diabetes by activating the anti-inflammatory reflex. *Nat. Med.* **20,** 484–492
46. Shi, S. Y., Lu, S. Y., Sivasubramaniyam, T., Revelo, X. S., Cai, E. P., Luk, C. T., Schroer, S. A., Patel, P., Kim, R. H., Bombardier, E., Quadrilatero, J., Tupling, A. R., Mak, T. W., Winer, D. A., and Woo, M. (2015) DJ-1 links muscle ROS production with metabolic reprogramming and systemic energy homeostasis in mice. *Nat. Commun.* **6,** 7415
47. Chen, C. T., Liu, Z., and Bazinet, R. P. (2011) Rapid de-esterification and loss of eicosapentaenoic acid from rat brain phospholipids: an intracerebroventricular study. *J. Neurochem.* **116,** 363–373